

Article

Instantaneous Quantum Description of Photonic Wavefronts and Applications

Andre Vatarescu

Fibre-Optic Transmission of Canberra, Canberra, Australia; email: andre_vatarescu@yahoo.com.au

Abstract: Three physical elements are missing from the conventional formalism of quantum photonics: 1) the quantum Rayleigh spontaneous and stimulated emissions; 2) the unavoidable parametric amplification; and 3) the mixed time-frequency spectral structure of a photonic field which specifies its duration or spatial extent. As a single photon enters a dielectric medium, the quantum Rayleigh scattering prevents it from propagating in a straight-line, thereby destroying any possible entanglement. A pure dynamic and coherent state composed of two consecutive number states, delivers the correct expectation values for the number of photons carried by a photonic wave front, its complex optical field, and phase quadratures. The intrinsic longitudinal and lateral field profiles associated with a group of photons for any instantaneous number of photons are independent of the source. These photonic properties enable a step-by-step analysis of the correlation functions characterizing counting of coincident numbers of photons or intensities with unity visibility interference, spanning the classical and quantum optic regimes.

Keywords: Quantum Rayleigh emissions; spatial fields of photons; photonic beam splitters and filters; photon coincidence counting; HOM dip with unity visibility

1. INTRODUCTION

Recent developments in the integration of photonic devices for quantum information processing [1] revolve around the concepts of one-photon and two-photon quantum interferences [2], both of which are predicated on a single photon propagating in a straight-line inside a dielectric medium. However, this assumption is totally undermined by the quantum Rayleigh scattering.

The quantum Rayleigh spontaneous and stimulated emissions were well documented four decades ago [3-4] when the first experimental results of apparently single photon propagation were incorporated in the theory of quantum optics. Even though the subject was revisited [5] to clearly find that the probability of spontaneous emission increases with the refractive index of the medium, the question of one single photon being scattered by photon-dipole interactions has been completely ignored in the professional literature of quantum optics [6].

One photon per radiation mode underpins the concept of entangled photons which, apparently, are needed to create a statistical correlation between separately measured quantum events of detection [2], [6]. Yet, the quantum Rayleigh scattering prevents a single photon from propagating in a straight line inside a dielectric medium [7-8]. Equally, inside a dielectric medium, the quantum Rayleigh stimulated emission can recapture an absorbed photon as well as coupling photons between two radiation modes, thereby creating groups of photons from individual photons [7-8], and forming pulses with a time-varying number of identical photons in a mixed time-frequency spectral structure [9].

The random phase of the spontaneously emitted photons is ignored [2] because number states do not carry an optical field. Instead, entangled states of one single photon are adopted as a way to deliver a non-zero interference term through outcome probability amplitudes. For instance, the path-entangled state $|\Psi_{AB}\rangle = \alpha |1\rangle_A |0\rangle_B + \beta |0\rangle_A |1\rangle_B$ describes a statistically quantum mixed state or global quantum wavefunction of two



Copyright: © 2022 by the authors. Submitted for possible open access publication under the terms and conditions of the Creative Commons Attribution (CC BY) license (<https://creativecommons.org/licenses/by/4.0/>).

possible pathways A and B , and as such, it can be used in any context, anywhere, and at any time. At the level of one single event and individual measurement, if only one photon propagates in the system at any given point in time, then the coefficients can only, instantaneously, be either $\alpha(t) = 1$ and $\beta(t) = 0$, or $\alpha(t) = 0$ and $\beta(t) = 1$. By contrast, the statistical average of the ensemble of measurements with a symmetric beam splitter would lead to an average of $\bar{\alpha} = \bar{\beta} = \sqrt{1/2}$ resulting in a non-zero interference term, even though for each and every component of the ensemble distribution, an instantaneous vanishing interference pattern is measured as the cross-term product is zero, i.e. $\alpha(t)\beta(t) = 0$, leading to a physical contradiction with the average non-zero value.

An average vanishing value for the product of two simultaneously sampled instantaneous photocurrents can arise by having positive and negative values of the electric levels with reference to a zero-value threshold, or by having each event returning a zero value. This physical and practical approach will do away with complicated and expensive single-photon sources and photodetectors because the mixed quantum state of the output wave packet from such sources corresponds *mathematically* to a time-independent source of simultaneous photons.

An ensemble distribution is built up from instantaneous measurements of photonic beam fronts. The instantaneous measurements require a wavefunction which changes with time and location to reflect the time- and space-dependence of the instantaneous values of the photonic beam, such as the number of photons, the complex-valued optical amplitude, and an exchange of energy with another wave front, as mediated by a photon-dipole interaction.

The interactions associated with quantum Rayleigh conversions of photons require a wavefunction capable of delivering transient or instantaneous expectation values for a pure state. The case for such states is presented in Section 2, and these states – labelled dynamic and coherent number states – are derived in Section 3 leading to the analysis of photonic coupling between radiation modes and waveguides. The description of the intrinsic field profiles of photons is presented in Section 4. Section 5 derives the detected interference patterns between fields of dynamic and coherent number states. The correct description of various beam splitters leading to intensity interference with unity visibility in the “classical” regime will be analyzed in Section 6.

2. THE PURE QUANTUM STATE OF MULTIPLE PHOTONS FOR INSTANTANEOUS MEASUREMENTS

The assumption that spontaneously emitted, parametrically down-converted individual photons cannot be amplified because of a low level of pump power would, in fact, prevent any emission in the direction of the phase-matching condition because of the Rayleigh spontaneous emission or scattering of photons.

A pure state delivers one single measurement [10-11], whereas a mixed state describes the statistical distribution of an ensemble of measurements [11]. A photonic wave front carries a number of photons across a dipole-hosting plane and its duration will be determined by the response time of the photon-dipole interaction [10].

Probability distributions of a physical, quantum process are built up by aggregating a large number of single event measurements into a statistical ensemble. Each photon-dipole interaction is driven by instantaneous values of number of photons and phase of the optical field. In other words, it is the pure state of the optical field at the level of a single, individual interaction that determines the instantaneous outcome, rather than a global wavefunction which is time- and space- independent.

It is pointed out in [12] that a quantum dot “emits a cascade of photons and a single photon is obtained only through *spectral filtering* of one emission line”. High-finesse optical cavities incorporated in a measurement setup distort the temporally regular sequence of single photons because of multiple internal reflections. The emerging stream may contain groups of a few overlapping photons, e.g. five, which may be unevenly split by a beam splitter and reduced in number through quantum Rayleigh spontaneous emission (QRSE) so as to generate no coincidence for a zero delay-time.

A mixed state of one-photon excitation as presented in [13, p. 8] is impractical for the description of the instantaneous quantum Rayleigh coupling of photons (QRCP) because the photon wave packet $|1\rangle_{j,\sigma}$ describes an output-measured and time-independent wave packet. "If the packet is dispersed spectrally by a prism and detected by an array of photon counters, only one counter will click, although which one clicks will be random. Such a state is expressed as $|1\rangle_{j,\sigma} = \int d^3k U_j^{(\sigma)}(\mathbf{k}) |1\rangle_{\mathbf{k},\sigma} / (2\pi)^{-3}$ where $|1\rangle_{j,\sigma}$ is a state with a single excitation having particular monochromatic wave vector-polarization state labeled by the pair (\mathbf{k}, σ) . We see that the function $U_j^{(\sigma)}(\mathbf{k})$ fully specifies the state." [13, p. 8]. This state is of no utility for evaluating the optical field involved in a dipole-photon interaction as the expectation values of the field operator \hat{a} vanish, ${}_{j,\sigma}\langle 1 | \hat{a} | 1 \rangle_{j,\sigma} = 0$. For the single-photon wave packet, only one radiation mode \mathbf{k} is taking part in the detection or photon coupling processes at a given point in time. Yet, an intrinsic photonic field distribution is carried by each interacting photon without any dependence on the measured statistical distribution of the ensemble of the mixed state.

3. PHOTONIC WAVE FRONT EXPECTATION VALUES AND DYNAMIC MOTION

As the number of photons and related field amplitude and phase carried by a photonic wave front may change as a result of the QRCP, the equations of motions for the corresponding expectation values will be evaluated with the Ehrenfest theorem [14-15].

Photons and their *instantaneous* properties are detected and measured by probing a sequence of wave fronts. The detection of photons occurs as a result of their optical field exchanging energy with electrons of the atomic structure of the detector, similarly to the Jaynes - Cummings model [6], [14] for the quantized dipole-photon exchange of energy.

3.1. The dynamic and coherent number states

Based on the formalism presented in [5], [16], the magnitude of the Poynting vector, i.e. the flux of energy \mathbb{F} (or number of photons / s) carried by an optical wave front of frequency ω and crossing a plane surface at position z is given in terms of the electromagnetic field magnitudes E and B , or corresponding operators, by the equalities:

$$\mathbb{F} = \omega \varepsilon [E^2 + c_m^2 B^2] = 0.5 \hbar \omega (a a^* + a^* a) \quad (1)$$

with $a = \sqrt{\varepsilon/\hbar} (E + i c_m B)$ and its complex conjugate a^* , ε and \hbar indicating the permittivity of the medium and the reduced Planck constant, respectively. The speed of light in the medium is $c_m = c/n_r = 1/(n_r \sqrt{\varepsilon_0 \mu_0})$, with n_r being the refractive index. From this relation one defines the annihilation and creation operators as:

$$\hat{a} = \sqrt{\varepsilon/\hbar} (\hat{E} + i c_m \hat{B}) \quad (2a)$$

$$\hat{a}^\dagger = \sqrt{\varepsilon/\hbar} (\hat{E} - i c_m \hat{B}) \quad (2b)$$

The free-space Hamiltonian \hat{H}_f is explicitly written as [5]:

$$\hat{H}_f = \hbar \omega \hat{N}_c \quad (3a)$$

$$\hat{N}_c = 0.5 (\hat{a}^\dagger \hat{a} + \hat{a} \hat{a}^\dagger) \quad (3b)$$

where \hat{N}_c is the symmetric and complete number operator and its eigenstates are the number states $|n\rangle$. The two terms of Eqs. (3) would have different eigenvalues. With the need for incremental increase or decrease of one photon per dipole-photon interaction, and, based on experimental results indicating that one photon is an indivisible amount of energy, we seek a wave function $|\Psi_n\rangle$ which will deliver the number of photons n from the following equalities, as well as a complex value for their optical field:

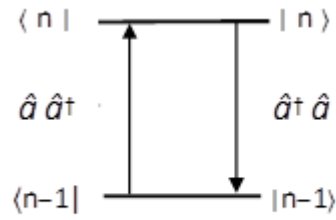


Fig. 1. An illustration of the dynamic and coherent two-component number states.

$$\langle \Psi_n | \hat{N}_c | \Psi_n \rangle = n \quad (4a)$$

$$\langle \Psi_n | \hat{a} | \Psi_n \rangle = (\langle \Psi_n | \hat{a}^\dagger | \Psi_n \rangle)^* = E e^{-i\varphi} \quad (4b)$$

$$\langle n | \hat{a}^\dagger \hat{a} | n \rangle = n; \text{ and } \langle n | \hat{a} \hat{a}^\dagger | n \rangle = n + 1 \quad (4c)$$

In Eq. (4c) the number states $| n \rangle$ are eigenfunctions, with different eigenvalues, of the two operator terms of \hat{N}_c .

The field operators \hat{a} and its adjoint \hat{a}^\dagger connect two consecutive number states, and consequently, a superposition of $| n-1 \rangle$ and $| n \rangle$ should give rise to a non-zero optical field for the following state vector:

$$|\Psi_n(t)\rangle = c_n(t) |n\rangle + c_{n-1}(t) |n-1\rangle \quad (5a)$$

$$|\Psi_n(t)\rangle = (|n\rangle + |n-1\rangle)/\sqrt{2} \quad (5b)$$

with the normalization condition of $|c_1(t)|^2 + |c_2(t)|^2 = 1$.

Analogously to the derivation [6] of coherent states of light $|\alpha\rangle$, the non-Hermiticity of the photon annihilation and creation operators allows for complex classical numbers (c -numbers) to be delivered when these operators act on number states. Applying \hat{a} and \hat{a}^\dagger to $| n \rangle$ returns a complex c -number

$$s_n = |s_n| \exp(-i\varphi_n) \quad (6)$$

which will become the complex amplitude of the state, so that:

$$\hat{a} | n \rangle = s_n | n-1 \rangle; \text{ and } \hat{a}^\dagger | n-1 \rangle = s_n^* | n \rangle \quad (7)$$

Recalling that \hat{a} and \hat{a}^\dagger are adjoint operators of each other, they interchange roles when acting on the Hermitian conjugate (or bra) states:

$$\langle n-1 | \hat{a} = s_n \langle n|; \text{ and } \langle n | \hat{a}^\dagger = s_n^* \langle n-1| \quad (8)$$

The condition for the number states being eigenstates of the number operator $\hat{N} = \hat{a}^\dagger \hat{a}$ requires that $|s_n|^2 = n$. The symmetric Hamiltonian of Eq. (3) suggests the two-component state vector of Eq. (5) as depicted in Fig. 1, and it carries out two simultaneous operations, one as a two-step number operator

$$\langle n | \hat{a}^\dagger \hat{a} | n \rangle = s_n s_n^* \quad (9)$$

and the second operation – illustrated in Fig. 1 – as a one-step transition operator between two consecutive number states, each operator acting on the state vector next to it (or the left-hand operators acting on the Hermitian conjugate wave functions $\langle n |$, the result being, for $|\Psi_n\rangle$ from (5b):

$$\langle \Psi_n | \hat{N}_c | \Psi_n \rangle = n \quad (10)$$

which is the number of photons carried by the wave front flux.

In the Heisenberg and Dirac interaction pictures, and using the retarded phase $\varphi = \omega t - z n/c$, the propagating photon field operators take the form [5], [14]:

$$\hat{a}(\omega, z, t) = \hat{a}(\omega) f(x, y, z) e^{-i(\omega t - \beta z)} \mathbf{e}_p \quad (11a)$$

$$\hat{a}^\dagger(\omega, z, t) = \hat{a}^\dagger(\omega) f(x, y, z) e^{i(\omega t - \beta z)} \mathbf{e}_p \quad (11b)$$

where the spatial distribution $f(x, y, z)$ is, conventionally, a solution of the Helmholtz wave equation [5] if there are enough photons to fill in the profile, and \mathbf{e}_p denotes the polarization of the radiation mode. Alternatively, the intrinsic field of photons will be derived in Section 4 below.

The observable quantity of the expectation value of the quadrature field operator $\hat{Q} = \hat{a} + \hat{a}^\dagger$ is found by combining Eqs. (2, 5-8, 11) to yield:

$$\langle \Psi_n(t) | \hat{a} | \Psi_n(t) \rangle = 0.5 e^{-i(\omega t - \beta z + \varphi(0))} \sqrt{n} e^{-i\varphi_n} \quad (12a)$$

$$\langle \Psi_n(t) | (\hat{a} + \hat{a}^\dagger) | \Psi_n(t) \rangle = \sqrt{n} \cos(\omega t - \beta z - \varphi_n) \quad (12b)$$

reproducing the c -number $\langle \hat{Q} \rangle$ corresponding to the "classical" optical field with a time-varying number of photons $n(t)$ and related phase $\varphi_n(t)$.

The correct expectation values can also be found for the phase quadrature operators [17]. These are defined in terms of the field operators and the conventional number operator $\hat{N} = \hat{a}^\dagger \hat{a}$, having the form, for $n > 0$:

$$\hat{C} = \hat{a} \hat{N}^{-1/2} + \hat{N}^{-1/2} \hat{a}^\dagger \quad (13a)$$

$$\hat{S} = i(\hat{a} \hat{N}^{-1/2} - \hat{N}^{-1/2} \hat{a}^\dagger) \quad (13b1)$$

4

which will provide information about the phase associated with the dynamic and coherent number states of Eqs. (5). With the photon number operator \hat{N} returning the number of photons in the basis of number states i.e., $\hat{N} |n\rangle = n |n\rangle$, any operator function $f(\hat{N})$ can be expanded in a power series and replaced in terms of the number of photons, as follows [6]: $F(\hat{N}) = \sum_p d_p \hat{N}^p$; $F(\hat{N}) |n\rangle = F(n) |n\rangle$; and $\hat{N}^{-1/2} |n\rangle = n^{-1/2} |n\rangle$ where d_p are expansion coefficients. For the particular case of the zero-photon state $|0\rangle$, the product operator needs to be inverted [17] by substituting $\hat{a} \hat{a}^\dagger = \hat{a}^\dagger \hat{a} + 1$ into the power series expansion of $\hat{a} f(\hat{N})$ to obtain $f(\hat{N}+1) \hat{a}$. The corresponding expressions for the expectation values are:

$$\langle \Psi_n | \hat{C}_j | \Psi_n \rangle = \cos(\omega t + \varphi_j) \quad (14a)$$

$$\langle \Psi_n | \hat{S}_j | \Psi_n \rangle = \sin(\omega t + \varphi_j) \quad (14b)$$

These relations of the field and phase quadratures apply to any number of photons spanning the entire range from the quantum regime of a few photons to the large number of photons characteristic of classical optical waves. Consequently, the quantum states of Eqs. (5) of dynamic and coherent number states allow for a smooth transition between the quantum and classical regimes. These variables will be measured by the method of balanced homodyne detection [10].

The dynamic and coherent number states identified in Eqs. (5) possess an optical field which can be compared with the classical field. Consequences of these properties are discussed in the following sub-Section.

3.2. The equations of motion of the optically linear parametric interactions

As an optical beam propagates through a dielectric medium, the magnitude and phase of the expectation value s_n may be modified by the simultaneous presence of another beam of photons of the same frequency. This effect is described by the Ehrenfest theorem [14-15]:

$$i \hbar \frac{\partial}{\partial t} \langle \Psi_n(t) | \hat{a} | \Psi_n(t) \rangle = \langle \Psi_n(t) | [\hat{a}, \hat{H}_{int}] | \Psi_n(t) \rangle \quad (15)$$

indicating that the expectation value of the optical field is modified by its commutator with the Hamiltonian of interaction \hat{H}_{int} .

Having identified a quantum wave function capable of delivering the instantaneous magnitude and phase of an optical field, we can now apply the formalism of [18-20] to the

propagation along an optical waveguide directional coupler by employing the following composite photonic quantum state function $|\Phi\rangle$ for two optical waves identified by their waveguide $|\Psi_{n,j}\rangle$ ($j = 1$ or 2), their Hamiltonian of interaction \hat{H}_{int} , and the equation of motion derived from (15):

$$|\Phi\rangle = |\Psi_{n,1}\rangle |\Psi_{n,2}\rangle \quad (16a)$$

$$\hat{H}_{int} = \hbar \omega \chi_q^{(1)} (\hat{a}_2^\dagger \hat{a}_1 + \hat{a}_2 \hat{a}_1^\dagger) \quad (16b)$$

$$\chi_q^{(1)} = (\hbar/\varepsilon) \chi^{(1)} \quad (16c)$$

where the real part of the first-order susceptibility of the dielectric medium $\chi_q^{(1)}$ includes the coefficient square linking the photon annihilation or creation operators and the electric field operator in eqs. (2). The Hamiltonian \hat{H}_{int} is derived from the interaction term $\mathbf{P}_2 \cdot \mathbf{E}_1^*$ of the Poynting vector [8, Eq. (2.4)]

The resultant equation of motion describing the mutual interaction is derived by substituting into Eq. (15) the relations of (16), yielding:

$$\frac{\partial}{\partial t} \langle \Phi | \hat{a}_1 | \Phi \rangle = -i \omega \chi_q^{(1)} \langle \Phi | \hat{a}_2 | \Phi \rangle \quad (17)$$

This interaction will modify the complex field amplitude $s_{n,j}$ of two co-propagating and overlapping optical beams of the same frequency, identifiable by their respective optical waveguides ($j = 1, 2$). From Eqs. (12a) we have for the expectation values of the optical fields

$$\langle \Phi | \hat{a}_j | \Phi \rangle = 0.5 e^{-i(\omega t + \varphi_j)} s_{n,j} \quad (18)$$

After converting to number of photons i.e., $|s_{n,j}|^2 = N_j$ and corresponding phases φ_j , the equation of motion (17) provides the rates of change of N_j and φ_j as follows:

$$\frac{\partial}{\partial z} N_1 = g_1 N_1 \quad (19a)$$

$$g_1 = -\kappa \left(\frac{N_2}{N_1} \right)^{1/2} \sin \theta_{21} \quad (19b)$$

$$\frac{\partial}{\partial z} \theta_{21} = (\beta_2 - \beta_1) + \kappa \left[\left(\frac{N_1}{N_2} \right)^{1/2} - \left(\frac{N_2}{N_1} \right)^{1/2} \right] \cos \theta_{21} \quad (19c)$$

$$\frac{\partial}{\partial z} \varphi_1 = \kappa \left(\frac{N_2}{N_1} \right)^{1/2} \cos \theta_{21} \quad (19d)$$

$$\kappa = \frac{1}{v_p} \frac{k_o}{2n} \iint dx dy \chi_q^{(1)} f_1 f_2 \mathbf{e}_1 \cdot \mathbf{e}_2 \quad (19e)$$

$$\theta_{21} = (\beta_2 - \beta_1) \cdot z + \varphi_2 - \varphi_1 \quad (19f)$$

where the gain coefficient g includes an overall coupling coefficient κ and depends on the polarization states \mathbf{e}_1 and \mathbf{e}_2 of the photons. The phase difference between the two waves is θ_{21} , β being the propagation constant and $z/t = v_p$ is the phase velocity. In (19e), k_o and n specify the free-space wavevector and the effective refractive index, respectively. It should be noted that equations (19) are identical to the classical ones of [8] describing the physically meaningful process of quantum Rayleigh conversion of photons. The coupling coefficient of Eq. (19e) indicates that the entire local value of the optically linear susceptibility $\chi^{(1)}$ is involved in the coupling process in the dielectric medium at any point where the two spatial distributions f_1 and f_2 overlap, each having units of m^{-1} , and the squares f_j^2 are normalized to a dimensionless unit over the cross-section area. This is in contrast to the physically questionable coupling between two optical waveguides apparently induced by a perturbation of the dielectric constant in the cladding.

Any two dynamic and coherent number states of (16a) co-propagating through a dielectric medium will couple photons from one state to the other depending on the relative phase between the two waves. This process, repeatedly, will eliminate optical waves whose phases diverge substantially from the phase of the surviving wave which will dominate the output of a lasing cavity.

Two groups of photons propagating simultaneously across the same dielectric medium would exchange photons, parametrically, with each other through the real part of the susceptibility – see Eqs. (19) above – which is indicative of a beam splitter composed of a waveguide directional coupler.

4. INTRINSIC FIELD PROFILES OF A PHOTONIC WAVE FRONT

The intrinsic longitudinal field profile of a group of photons, or its coherence length, can be calculated by using the wave function $|\Psi_n\rangle$ from (5b). Two equations can be identified for the expectation values of \hat{a} or the corresponding c -numbers, by combining (2) and (12a), leading to:

$$\langle \Psi_n | \hat{a} | \Psi_n \rangle = b \langle \hat{E} \rangle + i s \langle \hat{B} \rangle \quad (20a)$$

$$\langle \Psi_n | \hat{a} | \Psi_n \rangle = q e^{-i(\omega t - \beta z)} \quad (20b)$$

with $q = 0.5 \sqrt{n}$, $b = \sqrt{\varepsilon/\hbar}$, and, $s = c_m \sqrt{\varepsilon/\hbar}$. We point out that both quadratures of the field are represented in the phasor notation of Eqs. (20). From these equalities, the c -numbers of the electric and magnetic fields are denoted: $E = \langle \hat{E} \rangle$ and $B = \langle \hat{B} \rangle$. Recalling the relations [16] between the vector potential $\mathbf{A}(z, t)$ and the fields as:

$$\mathbf{E} = -\partial \mathbf{A} / \partial t \quad \text{and} \quad \mathbf{B} = \nabla \times \mathbf{A} \quad (21)$$

In the Cartesian frame of coordinates (x, y, z) , the vectors have the following notation, in the plane wave approximation:

$\mathbf{A} = (A, 0, 0)$; $\mathbf{E} = (E, 0, 0)$; $\mathbf{B} = (0, B, 0)$ and the wave vector is $\mathbf{k} = (ik_x, ik_y, \beta)$ for a beam propagating in the z -direction, in an optical waveguide. The complex amplitude of the vector potential is represented by

$$A(z, t) = A_p(z) f(x, y) e^{-i(\omega t - \beta z)} \quad (22)$$

where the lateral profile of the guided mode is given by $f(x, y)$ and the propagation constant by $\beta = 2\pi n_{eff} / \lambda$. The second term of the curl operation $\nabla \times f(x, y) \mathbf{x} = (\partial f / \partial z) \mathbf{y} - (\partial f / \partial y) \mathbf{z}$ does not lead to wave propagation and does not affect measurements in a plane perpendicular to the z -coordinate. The second term will therefore be set aside in the remainder of this analytic derivation.

Relating A_p to a moving source of photons would suggest a relative distance $\zeta = z - z_0$ with z_0 being the temporal location of the photons and the localization given by a Dirac delta function $\delta(z - z_0)$, resulting in this differential equation after substituting (21) and (22) into (20) to obtain:

$$\frac{\partial}{\partial z} A_p + \sigma A_p = \gamma \delta(z - z_0) \quad (23)$$

where $\sigma = b\omega/s + i\beta = (\omega/c)(n_r + i n_{eff})$ and $\gamma = -i q/s = -i 0.5 \sqrt{n} \sqrt{\hbar} / (c_m \sqrt{\varepsilon})$. Setting $A_p(z) = g(z) \exp(-\sigma z)$ and inserting into the differential equation (23) leads to: $\int dg = \gamma \int e^{\sigma z} \delta(z - z_0) dz$. With $g = \gamma e^{\sigma z_0}$, and for reasons of physical symmetry, the longitudinal distribution of the magnitude of the vector potential associated with photons of a wave front is found to be:

$$A_p(z) = \gamma \exp(-\sigma |z - z_0|) \quad (24a)$$

$$f_{ph}(z = ct) = \exp(-(2\pi |z - z_0|) n_r / \lambda) \quad (24b)$$

The vector potential's decay constant is inversely proportional to the wavelength λ through $Re \sigma = 2\pi n_r / \lambda$. Thus, the local optical field includes contributions from photons in the vicinity of z_0 , as illustrated in Fig. 2. The normalized longitudinal optical field

profile f_{ph} of one photon of wavelength λ , crossing point z_o , is obtained from (24b), and has the form of a Wigner spectral component $S(\omega, t)$, that is, a time-varying spectral component [9] – as opposed to a time-constant amplitude and phase of a Fourier spectrum – crossing a surface perpendicular to the wavevector of propagation. This exponential decay of the spatio-temporal profile is mistaken for that obtained by Fourier transforming a fully populated transmission line of an interference filter.

The longitudinal length of the intrinsic field in Eq. (24b) corresponds to the physical coherence length of one photon; the more photons there are in the group, the longer the coherence length becomes by superposition.



Fig. 2. Partially overlapping photonic fields.

The transversality condition [5] for a radiation field $\langle E \rangle \propto \langle \hat{a} + \hat{a}^\dagger \rangle$ and the dielectric constant ϵ , is given by the divergence of the displacement vector:

$$\nabla \cdot (\epsilon \mathbf{E}) = 0 \quad (25)$$

In cylindrical coordinates, this differential equation and its solution in the plane perpendicular to the wavevector are:

$$\frac{\partial}{\partial r} (r \epsilon \mathbf{E}) = 0; \quad \mathbf{E}(r) = \mathbf{E}_o \frac{r_o}{\epsilon r} \quad \text{or} \quad f_{ph,lat} = \frac{r_o}{\epsilon r} \quad (26)$$

where r_o is the reference position coordinate at the peak of \mathbf{E}_o , and $r = r_o + \Delta r$ is the distance from this position.

The coupling coefficient between two radiation modes will be modified below to take into account the longitudinal profile of the optical field given in (24b) and the lateral profile $f_{ph,lat}$ of (26), for the operation, as a beam splitter, of an optical waveguide directional coupler.

For the optical directional coupler, the evolution of the photons is governed by Eqs. (19) with the possibility of one waveguide capturing most of the photons resulting in an asymmetric output. The coupling coefficient κ will have to take into consideration the temporarily discrete nature of the groups of photons by including the longitudinal field profile f_{ph} next to the transverse spatial field $f = f_{ph,lat}$, that is:

$$\kappa = \frac{1}{v_p} \frac{k_0}{2n} \Gamma_{12}(z_o) \iint dx dy \chi_q^{(1)} f_1 f_2 \mathbf{e}_1 \cdot \mathbf{e}_2 \quad (27)$$

$$\Gamma_{12}(z_{o1}; z_{o2}) = \int_0^z f_{ph}(z - z_{o1}) f_{ph}(z - z_{o2}) dz$$

This spatio-temporal overlap is necessary for the quantum regime of discrete groups of photons. The phase-dependent coupling of photons of Eqs. (19) is critical in the operation of the optical waveguide beam splitters by creating, with the adjustable phase difference, an asymmetric output [21].

5. INTERFERENCE PATTERNS OF FIELDS OF DYNAMIC AND COHERENT NUMBER STATES

Another useful effect is the interference between two photonic beams reaching a photodetector. In the context of this analysis, one obtains that, in so far as localized and instantaneous detection of photons of two dynamic and coherent number states is concerned, the photocurrent $I_{ph}(t)$ generated by the interference output of a balanced

homodyne detector is calculated by combining the expectation values of the quadrature field operators given in Eq. (12) to obtain:

$$\langle I_{ph}(t) \rangle = K (\langle Q_a \rangle + \langle Q_b \rangle)^2 = K [N_a \cos^2(\xi_a) + N_b \cos^2(\xi_b) + 2 \sqrt{N_a N_b} \cos(\xi_a) \cos(\xi_b)] \quad (28)$$

with the constant of proportionality K corresponding to the quantum efficiency of photon-to-electron conversion. The phases are defined by $\xi_j = \omega_j t - \beta_j z - \varphi_j$ for $j = a$ or b . This approach of making use of initially evaluated expectation values links the quantum regime to the classical one. After time-averaging over a large number of optical frequency periods, namely, with the averaging time interval T satisfying $2\pi/\omega_j \ll T \ll 2\pi/|\omega_a - \omega_b|$, we find that $\langle \cos^2(\xi) \rangle = 1/2$, and $\langle \cos(\xi_1 + \xi_2) \rangle = 0$. Using the identity $\cos \xi_1 \cos \xi_2 = 0.5 [\cos(\xi_1 + \xi_2) + \cos(\xi_1 - \xi_2)]$ as well as $\langle \sin \xi \rangle = 0$, we retrieve the conventional interference pattern for the interval average:

$$\langle I(t)_{ph} \rangle = \frac{K}{2} \langle N_{tot}(t) [1 + \sigma \Gamma \cos(\xi_a(t) - \xi_b(t))] \rangle \quad (29)$$

$$\langle N(t) \rangle = \frac{1}{T} \int_{-T/2}^{T/2} N(t) dt; \text{ and } N_{tot}(t) = N_a(t) + N_b(t)$$

$$\sigma = \frac{2 \sqrt{N_a N_b}}{N_a + N_b} \hat{e}_a \cdot \hat{e}_b; \text{ and } \Gamma(\tau) = \frac{\int_0^T f_{ph}(t) f_{ph}(t + \tau) dt}{\int_0^T f_{ph}^2(t) dt}$$

where \hat{e}_j specifies the polarization of the group of photons, and the definition of the longitudinal overlap $\Gamma(\tau)$ follows from the longitudinal profile of photons of Eq. (24b). Equality (29) will be applied to two-detector correlations in the following Section. Thus, the formalism of this Section based on the intrinsic fields of photons leads to phase-dependent degrees of detections or detection probabilities of interfering groups of photons, enabling a smooth transition between the quantum and classical regimes for any level of optical power and any related phase. The statistical average can be evaluated in one step of a large number of photons or in a series of steps of small number of photons.

6. CORRELATIONS OF PHOTONS BY MEANS OF A DIELECTRIC INTERFACE BEAM SPLITTER

The analytic elements derived in the previous Sections will be applied hereafter. These elements are: the wave-function of (5) of the dynamic and coherent number states which deliver the correct expectation values for the number of photons carried by a photonic wave front and its associated complex amplitude in Eq. (12), and the optical field profile of a group of photons as shown in Eqs. (24b) and (26).

Given a photonic optical field, the Fresnel coefficients of reflection and transmission can be interpreted as probability amplitudes for the respective effects at a dielectric boundary [5]. These coefficients arise from the physical interactions at the dielectric interface, as opposed to the "black box" approach of having a phase difference of $\pm \pi/2$ between the reflection r and transmission t coefficients regardless of the structure of the beam splitter [6], [22]. The operations of dielectric beam splitters involve the quantum Rayleigh spontaneous and stimulated emissions. A symmetric Y-junction waveguide does not add any phase difference between the two pathways. As a result, for a 1x1 Mach-Zehnder interferometer, the detection probability for one single input photon $|r + t|^2$ could be larger than unity.

For a dielectric interface beam splitter as sketched in Fig. 3, with the arrows indicating the converging and diverging waveguides, the reflected and transmitted optical fields will lead to the transformation of the field operators based on Fresnel coefficients:

$$\hat{a}_c^\dagger = -r_1 \hat{a}_a^\dagger + t_1 \hat{a}_b^\dagger \quad \text{and} \quad \hat{a}_d^\dagger = t_2 \hat{a}_a^\dagger + r_2 \hat{a}_b^\dagger \quad (30)$$

where the subscripts of the reflection r and transmission t coefficients indicate the exiting direction of the photons.

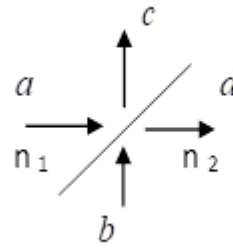


Figure 3. A typical dielectric interface beam splitter. Photons arrive simultaneously at the diagonal boundary interface $n_2 > n_1$. The arrows correspond to converging and diverging waveguides of an X-junction.

To illustrate an application of this approach, two groups of photons generated independently as the input signal a and signal b are impinging, from opposite sides, on the integrated optical beam splitter of Fig. 3 which is placed in the $x y$ plane, with $|r| = |t| = \sqrt{0.5}$. The dielectric boundary is used as the synchronization place, i.e. $\tau = 0$ for the time delay τ between the two groups of photons. Time-shifts of opposite signs $\pm \tau$ for the arrival at the interface of the two groups of photons may be added by controlling locally the refractive index or the propagating distance. The relative phases of these photonic wave fronts in the directions of the c and d waveguides are, for photodetector PD1, and photodetector PD2, respectively:

$$\text{For PD1: } \xi_{ar}(t, \tau) = -\omega \tau + \varphi_a(t) - \pi \text{ and } \xi_{bt}(t) = \varphi_b(t) \quad (31a)$$

$$\text{For PD2: } \xi_{at}(t) = \varphi_a(t) \text{ and } \xi_{br}(t, \tau) = \omega \tau + \varphi_b(t) \quad (31b)$$

where the random phases of the spontaneously emitted photons are denoted by $\varphi(t)$ and a $(-\pi)$ phase shift is due to the upwards reflection. Any bias phases may be included in $\varphi(t)$.

The combined number of photons $N_j(t)$ detected by photodetector $j=1; 2$ is evaluated from the interference pattern of the instantaneously measured flux of photons presented above in Eqs. (29), with the phases given by Eqs. (31).

The correlation function $C_{12}(\tau)$ between two photocurrents $I(t)_{ph,j}$ generated by independent streams of photons and detected by two separate photodetectors, is specified by the following averaging relation for independent sources and detections:

$$\begin{aligned} C_{12}(\tau) &= \langle I(t)_{ph,1} I(t + \tau)_{ph,2} \rangle = \\ &= \langle I(t)_{ph,1} \rangle \langle I(t + \tau)_{ph,2} \rangle \end{aligned} \quad (32)$$

We shall illustrate the possibility of “classical” unity visibility by assuming $\sigma = 1$ and $\Gamma(0) = 1$ in Eq. (29) to obtain the normalized correlation function as the probability of joint detection P_{12} for independent detection probabilities for steady and controllable phases ϕ_1 and $\phi_2 \in \{0; 2\pi\}$:

$$\begin{aligned} P_{12}(\phi_1; \phi_2) &= P_1(\phi_1)P_2(\phi_2) = \frac{C_{12}}{K^2 N_{tot;1} N_{tot;2}} = \\ &= \frac{1}{4}[1 + \cos \phi_1 + \cos \phi_2 + \cos \phi_1 \cos \phi_2] \\ &= \frac{N_{ph;1}(\phi_1) N_{ph;2}(\phi_2)}{N_{tot;1} N_{tot;2}} \end{aligned} \quad (33)$$

where $\phi_j = \xi_{aj} - \xi_{bj}$ is the phase difference for interference at photodetector $j=1; 2$. The third line of Eq. (33) describes the experimental parameters with the number of detected photons being $N_{ph;j}$ and the total number of incoming photons per photonic group identified as $N_{tot;j}$.

With one photonic group undergoing a $-\pi$ phase shift upon reflection at the interface with a higher refractive index of the dielectric medium, and all photons propagating the same distance or having the same bias phase, the second and third terms on the second line of Eq. (33) become $\cos \phi_1$ and $\cos(\phi_1 + \pi)$ as $\phi_1 - \phi_2 = -\pi$, and cancel each other out for each individual measurement of the ensemble. This is the case of $N_{ph,1} = 0$ leading to $P_{12}(\phi_1; \phi_2) = 0$ for any number of photons. An enhanced sensitivity to phase modulation in the case of intensity correlation can be found from Eq. (33) by setting $\cos \phi_1 = 1$ and $\cos(\phi_2 + \pi/2) \approx -\phi_2$ leading to a variation of $2\phi_2$. The two intensity sets of interference patterns can also be generated separately and their sampled values multiplied to give rise to Franson-type correlations [2] with controlled phases as follows.

The coincidence counting of photons for the transient interference patterns of the two separate photodetector intensities, over the coincidence time interval T (a few ns) is also derived from Eq. (33), for a group of amplified spontaneously emitted photons such as the signal and idler photons of a parametric source. The result will be the aggregate of $\langle P_{12}(\phi_1; \phi_2) \rangle$ over the entire range of $\{0; 2\pi\}$. From $\cos \phi_1 \cos \phi_2 = 0.5 [\cos(\phi_1 + \phi_2) + \cos(\phi_1 - \phi_2)]$, the first term on the right-hand side vanishes upon integration over the range $\{0; 2\pi\}$ of random phases, and the correlation of intensities is evaluated from Eqs. (33) to be:

$$P_{12} = \{1 + \cos[(\omega_b - \omega_a)\tau - \pi]\}/4 \quad (34)$$

after realizing that there are two statistical possibilities for the random phases $\varphi_a(t)$ and $\varphi_b(t)$ of the spontaneously emitted photons. The random phases from the two photocurrents cancel each other out but these two random phases $\varphi_a(t)$ and $\varphi_b(t)$ can interchange values without affecting the result, and the cosine term of $0.5 \cos(\phi_1 - \phi_2)$ should be counted twice when calculating, "classically", the correlation function $P_{12}(\tau)$. Alternatively, we recall that the contributions from the second and third terms on the second line of Eq. (33) add up to zero by integrating over the phase interval of $\{0; 2\pi\}$ while the last term of the interference becomes $\cos \phi_1 \cos \phi_2 = -\cos^2 \phi$ and its contributions cover two periods of π rad with positive values adding up to unity. From (34), for $\tau = 0$, we find a vanishing correlation probability $P_{12} = 0$, which corresponds to the Hong–Ou–Mandel (HOM) dip. This is consistent with the experimental correlations with uncorrelated photons [23].

For the case of photons from two optical sources reaching, simultaneously, two separate photodetectors, the probability of joint detections [24] or intensities correlation is evaluated by removing the $-\pi$ phase from Eq. (34) to obtain, for complete overlap, twice the probability $P_{12}(\Gamma = 1) = 2 P_{12}(\Gamma = 0)$, [24] of separate detections, which is characteristic of the original Hanbury Brown & Twiss experiment.

Next, we recall the parametric phase-pulling effect [19] leading to a phase correlation between the signal and the idler waves, i.e. $\varphi_s + \varphi_i = \varphi_p + \pi/2$, for any initial phases of weak waves such as spontaneous emission, with the coherent phase of the pump photons given by φ_p , to find a constant phase relation $\phi_1 + \phi_2 = \varphi_{sa} - \varphi_{sb} + \varphi_{ia} - \varphi_{ib} = \varphi_{pb} - \varphi_{pa}$ for the $\cos(\phi_1 + \phi_2)$ term above, which points out the role played by the relative pump phases. This phase relation will result in nonvanishing intensity correlations in the case of a 2×2 Mach-Zehnder interferometer [21], as well as for two-source experiments outlined in ref. [2], doing away with quantum mysteries.

7. CONCLUSION

The conventional interpretation of one-photon per radiation mode fails to consider the quantum Rayleigh scattering and stimulated emission, as well as the unavoidable parametric amplification of spontaneously emitted photons. An analysis focused on time- and space- dependent pure quantum states describing single and independent events of propagation, photon-dipole interactions and photodetections reveals physical processes and new features such as the dynamic and coherent number states for phase-dependent, instantaneous coupling of photons, the intrinsic longitudinal and lateral fields of photons,

a smooth transition from a low number to a high number of interfering photons, and the possibility of a unity visibility in the “classical” regime with Fresnel coefficients.

References

- [1] Moody, G. *et al*, “2022 Roadmap on integrated quantum photonics”, **2022**, *J. Phys. Photonics*, **4**, 012501.
- [2] Mandel, L. “Quantum effects in one-photon and two-photon interference,” **1999**, *Rev. Mod. Phys.*, **71**, S274-S282.
- [3] W. H. Louisell, W. H. *Quantum Statistical Properties of Radiation*, **1973**, John Wiley & Sons.
- [4] Marcuse, D. *Principles of Quantum Electronics*, **1980**, Academic Press.
- [5] Glauber, R. J. and Lewenstein, M. “Quantum optics of dielectric media,” **1991**, *Phys. Rev. A*, **43**, 467- 491.
- [6] Garrison, C. and Chiao, R. Y. *Quantum Optics*, **2008**, Oxford University Press.
- [7] Vatarescu, A. “The Scattering and Disappearance of Entangled Photons in a Homogeneous Dielectric Medium,” **2019**, *Rochester Conference on Coherence and Quantum Optics (CQO-11)*, doi.org/10.1364/CQO.2019.M5A.19.
- [8] Vatarescu, A. “Photonic coupling between quadrature states of light in a homogeneous and optically linear dielectric medium,” **2014**, *J. Opt. Soc. Am. B*, **31**, 1741–1745.
- [9] Cohen, L. “Time-frequency distributions-a review,” **1989**, *Proc. IEEE*, **77**, 941–981.
- [10] Breitenbach, G., Schiller, S., and Mlynek, J. “Measurement of the quantum states of squeezed light,” **1997**, *Nature*, **387**, 471-475.
- [11] Fano, U. “Description of States in Quantum Mechanics by Density Matrix and Operator Techniques,” **1957**, *Rev. Mod. Phys.*, **29**, 74-93.
- [12] Senellart, P., Solomon, G. and White, A. “High-performance semiconductor quantum-dot single-photon sources,” **2017**, *Nature Nanotech.*, **12**, 1026-1039,.
- [13] Smith, B. J. and Raymer, M. G. “Photon wave functions, wave-packet quantization of light, and coherence theory”, **2007**, *New J. Phys.*, **9**, 414.
- [14] Steck, D. A., *Quantum and Atom Optics*, University of Oregon, available online at <http://steck.us/teaching> (revision 0.11.0, 18 August 2016).
- [15] Griffiths, D. J., *Introduction to Quantum Mechanics*, **2005**, Publisher: Pearson Prentice Hall.
- [16] Blow, K. J., Loudon, R., Phoenix, S. J. D. and Shepherd, T. J., “Continuum fields in quantum optics,” **1990**, *Phys. Rev. A*, **42**, 4102-4114.
- [17] Carruthers, P. and Nieto, M. M., “Phase and Angle Variables in Quantum Mechanics,” **1968**, *Rev. Mod. Phys.*, **40**, 411-440.
- [18] Vatarescu A, “Phase-Sensitive Amplification with Low Pump Power for Integrated Photonics, **2016**, “OSA Advanced Photonics Congress, paper ID: IM3A.6.
- [19] Vatarescu, A., “Photonic Quantum Noise Reduction with Low-Pump Parametric Amplifiers for Photonic Integrated Circuits”, **2016**, *Photonics*, **3**, 61.
- [20] Vatarescu, A., “Instantaneous Quantum Description of Photonic Wavefronts for Phase-Sensitive Amplification,” **2018**, *Frontiers in Optics/Laser Science Conference (FiO/LS)*, paper JW4A.109, Washington.
- [21] Kim, H., Lee S. M. and Moon, H. S. “Two-photon interference of temporally separated photons”, **2016**, *Sci. Rep.*, **6**, 34805.
- [22] Kim, Y. S., Slattery, O., Kuo, P. S. and Tang, X. “Two-photon interference with continuous-wave multi-mode coherent light”, **2014**, *Opt. Express*, **22**, 3611-3620.
- [23] Kim, H., Kwon, O. and Moon, H. S., “Experimental interference of uncorrelated photons”, **2019**, *Sci. Rep.*, **9**, 18375.
- [24] Iannuzzia, M., Francini, R., Messi, R. and Moricciani, D. “Bell-type Polarization Experiment With Pairs Of Uncorrelated Optical Photons”, **2020**, *Phys. Lett. A*, **384** (9), 126200.